Surrogate Model Development for Fuels for Advanced Combustion Engines

K. Anand,[*,†] Y. Ra,[†] R. D. Reitz,[†] and B. Bunting[‡]

[†]Engine Research Center, University of Wisconsin—Madison, Madison, Wisconsin 53706, United States

[‡]Oak Ridge National Laboratory, Oak Ridge, Tennessee 37831, United States

ABSTRACT: The fuels used in internal-combustion engines are complex mixtures of a multitude of different types of hydrocarbon species. Attempting numerical simulations of combustion of real fuels with all of the hydrocarbon species included is highly unrealistic. Thus, a surrogate model approach is generally adopted, which involves choosing a few representative hydrocarbon species whose overall behavior mimics the characteristics of the target fuel. The present study proposes surrogate models for the nine fuels for advanced combustion engines (FACE) that have been developed for studying low-emission, high-efficiency advanced diesel engine concepts. The surrogate compositions for the fuels are arrived at by simulating their distillation profiles to within a maximum absolute error of ~4% using a discrete multi-component (DMC) fuel model that has been incorporated in the multi-dimensional computational fluid dynamics (CFD) code, KIVA-ERC-CHEMKIN. The simulated surrogate compositions cover the range and measured concentrations of the various hydrocarbon classes present in the fuels. The fidelity of the surrogate fuel models is judged on the basis of matching their specific gravity, lower heating value, hydrogen/carbon (H/C) ratio, cetane number, and cetane index with the measured data for all nine FACE fuels.

1. INTRODUCTION

The continuous need to improve the efficiency and emissions of internal-combustion engines requires optimization of the entire fuel/engine/after-treatment system.[1,2] The impact of fuel composition and property changes on engine efficiency and emissions is a key research area for the design and development of engines and fuels. Research focus has intensified more recently with the introduction of advanced diesel engine concepts, such as low-temperature combustion (LTC), homogenous charge compression ignition (HCCI), etc., whose combustion process is highly sensitive to fuel composition and property changes and whose combustion process control is difficult to achieve.[3,4]

The fuels for advanced combustion engines (FACE) have been developed in a joint project between the U.S. Department of Energy and the Co-ordinating Research Council (CRC), which is a research body composed of automobile, engine, and energy companies for studying advanced combustion engine concepts,[5] among many problems of relevance. The mission of the FACE working group is to recommend a set of test fuels that are well-suited for research, so that the researchers evaluating advanced combustion systems may compare results from different laboratories using the same set of fuels for consistency.[6] The FACE working group has identified three major properties, viz., cetane number (measure of ignition quality), aromatic content (measure of fuel chemistry) and 90% distillation temperature (measure of volatility), that are of primary importance in deciding the performance of advanced combustion engines.[5,7−9] A matrix of eight fuels with two different target levels of these three properties, viz., cetane numbers of 30 and 55, aromatics of 20 and 45 vol %, and 90% distillation temperatures of 270 and 340 °C, was built around a center fuel with a target cetane number of 42.5, aromatics of 32.5 vol %, and 90% distillation temperature of 305 °C.[8]

Numerical simulations of the spray and combustion processes of fuels in internal-combustion engines using multi-dimensional computational fluid dynamics (CFD) codes, such as KIVA-3V, require accurate values of the fuel properties, including density, vapor pressure, surface tension, latent heat of vaporization, liquid- and vapor-phase specific heat capacity, viscosity, and thermal conductivity over a range of temperatures from the ambient condition to above the critical temperature conditions.[10] Experimental determination of these fuel properties at varying temperature conditions is difficult, especially at very high temperatures. Hence, it is important to accurately estimate the fuel properties for carrying out spray and combustion simulation studies of the real fuels. Further, accurate chemical kinetic modeling to describe the fuel−air gas-phase oxidation reactions is crucial to the development and improvement of advanced combustion engine operations, such as HCCI.[11,12] Because some transportation fuels may include thousands of hydrocarbon compounds,[11,13] theoretical investigations of spray and combustion processes of these fuels can only be realized with representative surrogate fuel models.

The present work proposes surrogate fuel compositions for the nine FACE fuels by modeling their distillation profiles, such that the chosen surrogate compositions cover the range and measured concentrations of the various hydrocarbon classes in the fuels, and also represents properties important for modeling spray and combustion processes. It should be noted that the composition and property surrogate models discussed in the present work are a part of an overall approach to simulate the combustion process of realistic fuels using multi-component reduced reaction

Table 1. Summary of Existing Surrogate Models for Diesel and Gasoline Fuels

reference	surrogate hydrocarbon species	target applications
15	n-decane, iso-octane, methylcyclohexane, and toluene	premixed diesel combustion
12	n-heptane and toluene	diesel ignition under HCCI engine conditions
22	n-decane, n-butylcyclohexane, and n-butylbenzene	properties, composition, and reactivity of diesel fuel
27	n-tetradecane	diesel spray and vaporization
	n-heptane	diesel combustion
21	n-tetradecane, n-decane, heptamethylnonane, and 1-methyl naphthalene	diesel spray and combustion
23	cyclohexane, decalin, toluene, n-decane, n-dodecane, n-tetradecane, n-hexadecane, and n-octadecane	diesel spray
	cyclohexane, toluene, n-heptane, and n-tetradecane	diesel combustion
28	iso-octane, n-heptane, toluene, methyl cyclohexane, and 1-pentene	gasoline ignition and gas-phase oxidation
29	n-heptane, iso-octane, and toluene	gasoline HCCI combustion
27	n-heptane, iso-octane, iso-hexane, 1-hexene, and toluene	gasoline properties, combustion, and emission

mechanisms. The requirement of a large number of surrogates (∼14) to accurately simulate the composition and properties of the fuels may prohibit the inclusion of all of the surrogates in chemical reaction mechanisms for studying the gas-phase oxidation of the fuels, even if mechanisms were available for each surrogate (which they are not, at least for most of the surrogates considered in this work). Hence, a hybrid surrogate modeling approach is proposed, wherein the physical properties of the fuels are represented by a "physical property" surrogate model, as in the present study, and a separate "chemistry" surrogate model (with fewer representative hydrocarbon species) is used to describe the gas-phase oxidation of the fuel. The concentrations of the hydrocarbon species from the fuel property model could be distributed to the fuel oxidation surrogates based on chemical class grouping. This paper focuses on accurately matching chemistry class, distillation, and physical properties. The subject of matching chemistry will be the subject of a second paper.

2. STATE-OF-THE-ART

A surrogate fuel is defined as a fuel composed of a smaller number of known concentrations of selected pure compounds whose behavior matches certain characteristics of the target fuel.[14,15] Scrutiny of the existing literature on surrogate fuel model development reveals that the representation of real fuels by surrogates has been practiced for many decades,[16] and a large number of surrogates have been proposed for jet fuels, as compared to the other transportation fuels.[17−19] Surrogates have been used to replace the real fuels in computational models as well as in experiments. Certain guidelines are available for the choice of surrogates based on their intended applications, as follows: feasibility (known chemical kinetic mechanism), simplicity (computational capability), similarity (real fluid physical and chemical properties, viz., density, heating value, evaporation characteristics, chemical composition, C/H ratio, and ignition delay), cost, and availability.[11,20]

The surrogates are proposed to mimic the real fuel properties, including ignition, combustion, and emission characteristics. Thus, the surrogates have a wide range of application targets, and a surrogate tailored for modeling, say, the ignition process, can be different from a surrogate applied for soot modeling.[11] A large number of surrogate models have been proposed for chemical kinetic modeling, targeting primarily the ignition behavior of the fuel.[12,21] The development of a surrogate mixture, which can mimic both the physical properties and the combustion

Table 2. Measured Hydrocarbon Classes in FACE Fuels by Mass Spectrometry[7] (% Mass)

hydrocarbon type/FACE fuel	1	2	3	4	5	6	7	8	9
paraffins	61.3	64.8	31.4	39.7	52.2	42.1	47.9	41.7	34.0
total napthenes	14.7	15.5	25.6	22.8	29.9	37.9	16.3	17.1	34.0
total saturates	76.0	80.3	57.0	62.5	82.1	80.0	64.2	58.8	68.0
alkylbenzenes	22.4	18.5	37.2	35.8	16.8	15.5	33.3	17.7	26.4
polynulear aromatics	1.5	1.2	5.8	1.7	1.0	4.6	2.5	23.6	5.5
tetralins	0.8	0.7	7.5	0.6	2.9	6.0	0	4.0	6.9
total aromatics	23.9	19.7	43.0	37.5	17.8	20.1	35.8	41.3	31.9

and sooting tendency of a real fuel, is a most difficult goal and would require blending more complex components.[16,22] To overcome this problem, a hybrid modeling methodology involving one surrogate model to represent the fuel spray, vaporization, and gas flow transport calculations and a separate surrogate model for gas-phase oxidation has been found to be effective.[21,23]

A sensitivity analysis on the effect of 11 different thermophysical properties on ignition delay and burning rate estimates identified that the simulation results are most sensitive to liquid density variations, primarily because of their effect on the mixture preparation process.[24] Among the different physical and chemical properties of a fuel, the following properties have been identified as most important for the surrogate fuel formulation: (i) carbon/hydrogen ratio,[15,20] because of its effect on local mixing phenomena in terms of the stoichiometry in diesel fuel applications, (ii) density,[15,20] because of its influence on atomization and mixing processes, (iii) higher heating value,[20] which is related to the fuel energy release, (iv) distillation,[20,25] which represents fuel volatility characteristics, (v) and finally, ignition characteristics,[12,16,21] which are significant in HCCI and LTC combustion applications. The thermo-physical properties, such as specific heat capacity, latent heat of vaporization, and thermal conductivity of petroleum products, are closely related to their density and can be accurately estimated if their fuel density is known a priori.[26]

Example surrogate models in the literature for representing diesel and gasoline fuels are summarized in Table 1. The summary reveals that the surrogates to represent diesel fuel vary to a greater extent even for the same target application. Also observed is that the total number of surrogate species required to model the fuel properties is relatively higher compared to the number used for modeling the ignition and combustion kinetics.
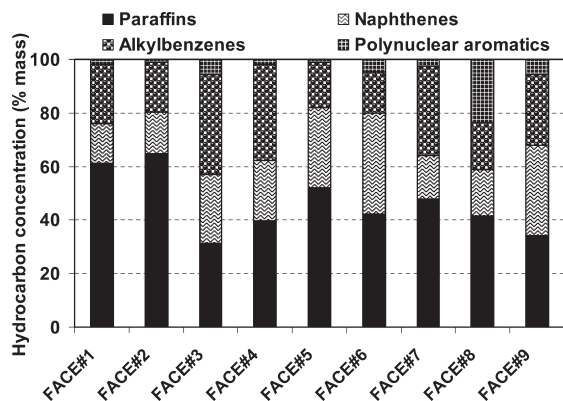
Figure 1. Measured hydrocarbon class distribution in FACE fuels.[7]
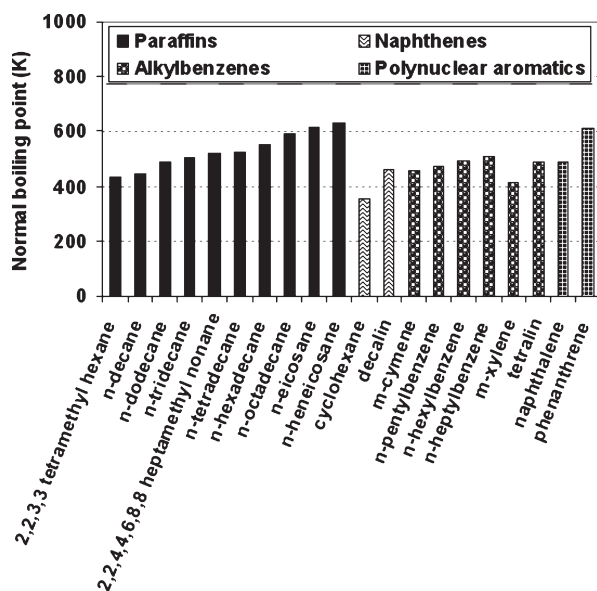

Figure 2. Variations in normal boiling point of chosen surrogate species.[34]

The scope of the present work involves developing suitable surrogate models for representing the composition and properties of the nine FACE fuels based on their measured hydrocarbon classes and distillation profiles.

3. METHODOLOGY

Much attention has been paid to the distillation characteristics of multi-component fuels because this can give valuable information about the performance in engine applications, such as evaporative emissions, cold start, warm-up, combustion deposit, oil contamination, combustion efficiency, etc.[30] The distillation or preferential vaporization of a multi-component fuel solely depends upon its composition, and the distillation profile of a fuel is a graphical depiction of boiling temperature against the volume fraction distilled. Because the distillation profile of each FACE fuel is determined by its composition, it is intended to model the distillation profiles of the FACE fuels using suitable surrogate compositions. For this purpose, the initial step involves identification of suitable hydrocarbon species for inclusion in the surrogate mixtures based on their boiling points. The measured hydrocarbon classes of the nine FACE fuels obtained by mass spectrometry based on American Society for Testing and Materials (ASTM) D2425[7] is provided in Table 2 and Figure 1. It is observed that, although the FACE fuels are

complex mixtures of hundreds to thousands of hydrocarbon compounds, they can be grouped into three main hydrocarbon classes, viz., paraffins, naphthenes, and aromatics. From this data, a list of representative hydrocarbon compounds was constructed, as shown in Figure 2, covering the range of measured hydrocarbon classes and also the minimum and maximum boiling range of all of the nine FACE fuels. It should be noted that, although *n*-paraffins and iso-paraffins are lumped as paraffins in the measured hydrocarbon classes in the nine fuels, the two iso-paraffins, viz., tetramethyl hexane ($C_{10}H_{22}$) and heptamethyl nonane ($C_{16}H_{34}$), are considered for the low cetane fuels (FACE 1, 2, 3, and 4), primarily to improve the cetane number predictions.

A discrete multi-component (DMC) fuel model[31] representing the properties and composition of multi-component fuels and incorporated in the multi-dimensional CFD code, KIVA-ERC-CHEMKIN, was used to simulate the distillation profiles of each fuel. The code is a modified version of the KIVA-3V, release 2, code with improved submodels developed at the Engine Research Center[31,32] and coupled with the chemical kinetics code CHEMKIN II[33] for detailed chemistry calculations. All of the thermophysical properties of the representative hydrocarbon species were taken from Daubert and Danner[34] and were incorporated in the fuel library of the code. A brief review of the discrete multi-component vaporization model and the method of estimation of distillation profiles are presented next.

3.1. Vaporization Model. The droplet vaporization model[31] considers the evaporation of spray droplets using the discrete multi-component (DMC) approach under the temperature range from flash-boiling conditions to normal evaporation. The improved model accounts for variable internal droplet temperatures and considers an unsteady internal heat flux with internal circulation and a model for the determination of the droplet surface temperature. The model uses an effective heat-transfer coefficient model for the heat flux from the surrounding gas to the droplet surface. Also, the variable density of the diesel-surrogate fuel as a function of the temperature is considered in the governing equations and the relevant submodels. The effective heat-transfer coefficient calculated in the model is also used to determine the amount of fuel to be treated as vapor when the drop surface temperature reaches the critical temperature (mass averaged value from those of pure components), while the drop interior is still in the subcritical condition. Its theoretical formulation is briefly discussed next.

3.2. Liquid-Phase Balance Equation. The liquid-phase species can be approximated as being well-mixed because the mass-transfer rates of the fuel components in the liquid droplets are so large.[35] However, a surface temperature model is introduced because of the finite heat-transfer rate.

A general form of the governing equation for the change in the liquid fuel distribution is

$$\frac{\mathrm{d}}{\mathrm{d}t}\left(y_{i,l}\rho_l \frac{4}{3}\pi R^3\right) = \dot{m}_i 4\pi R^2 \tag{1}$$

where $y_{i,l}$ is the mass fraction of species i in the liquid, ρ_l is the mass density of the liquid fuel, R is the droplet radius, and $\dot{m}_i$ is the vaporization rate of species i per unit surface area. The finite difference form of eq 1 during a given time step Δt is
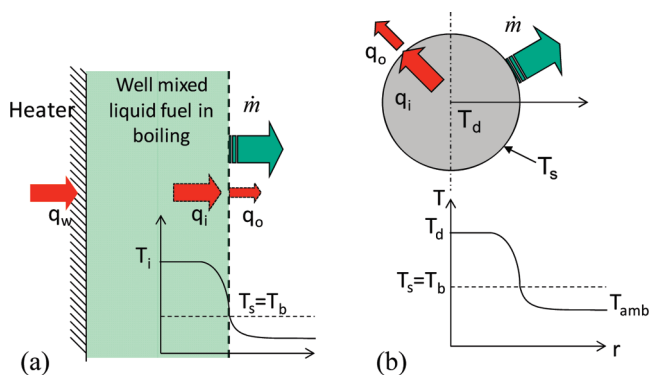
$$y_{i,l,2}\rho_{l,2}\frac{4}{3}\pi R_2{}^3 = y_{i,l,1}\rho_{l,1}\frac{4}{3}\pi R_1{}^3 - \dot{m}_i 4\pi R_1{}^2\Delta t \tag{2}$$

where the subscripts 1 and 2 denote the beginning and ending states of the drop, respectively.

The change of liquid drop energy is obtained from the conservation equation of energy for the two-phase system consisting of the drop and the surrounding gas mixture as

$$\frac{\mathrm{d}}{\mathrm{d}t}\left(\int_0^R c_{v,l}\rho_l 4\pi r^2 T(r)\mathrm{d}r\right) = \frac{\mathrm{d}}{\mathrm{d}t}\left(c_{v,l}\rho_l\frac{4}{3}\pi R^3 T_d\right)$$

$$= 4\pi R^2(q_i - \dot{m}c_{v,l}T_s) \tag{3}$$

Figure 3. Schematic configuration of the temperature and heat flux in distillation: (a) batch distillation process and (b) droplet evaporation in flash boiling conditions.

where $c_{v,l}$ is the specific heat of the liquid fuel, q_i is the heat-transfer rate from the drop surface to the interior per unit area, and T_d and T_s are the average drop temperature and surface temperature, respectively. The finite difference form of eq 3 during a given time step Δt is

$$c_{v,l,2}\rho_{l,2}\frac{4}{3}\pi R_2{}^3 T_{d,2} = c_{v,l,1}\rho_{l,1}\frac{4}{3}\pi R_1{}^3 T_{d,1}$$
$$+ 4\pi R^2(q_i{}^* - \dot{m}c_{v,l}T_s{}^*)\Delta t \tag{4}$$

where $q_i{}^*$ and $T_s{}^*$ mean values of the heat-transfer rate and the drop surface temperature, respectively, during the time step Δt.

3.3. Governing Equations for the Gas Phase. The conservation equation of species in the gas phase is

$$\frac{\partial}{\partial t}[\rho y_i] + \nabla[\rho y_i v] = \nabla(\rho D_i \nabla y_i) + s_{g,i} \tag{5}$$

where v and ρ are the velocity and density of the gas mixture, respectively, y_i and D_i are the mass fraction and diffusion coefficient of species i, and $s_{g,i}$ is the source term.

The energy conservation equation for the gas phase is

$$\overline{C}_P\frac{\partial}{\partial t}(\rho T) + \overline{C}_P\nabla(\rho v T) = \nabla\lambda\nabla T + (C_{PF}\overline{D}_F - C_{PA}\overline{D})\rho\nabla y_F\nabla T \tag{6}$$

where T is the temperature, λ is the thermal conductivity, $\overline{C}_P$ is the mixture specific heat, C_{PA} is the specific heat of air, and $\overline{C_{PF}D_F}$ is the average value of the product of specific heat and the diffusion coefficient of the fuel species. The last term in eq 6 represents energy transport because of interdiffusion of species.

3.4. Surface Temperature Estimation. The surface temperature of the droplet is determined from a heat- and mass-transfer balance at the interface between the droplet and the surrounding gas. There are two regimes of heat transfer, i.e., heat transfer occurring from the inside of the droplet to the surface, q_i, and heat transfer occurring from the outer gas to the surface, q_o. The rate of heat transfer balances the required heat for vaporization at the surface

$$L(T_s)\dot{m} = q_i + q_o \tag{7}$$

where $L(T_s)$ is the latent heat of the fuel at the surface temperature, T_s, and $\dot{m}$ is the mass vaporization rate.

Using appropriate models for internal and external heat transfer at a quasi-steady condition that considers the effects of interdiffusion and

Stefan flow, an explicit equation that relates the vaporization rate, $\dot{m}$, to the temperatures of the droplet and the surrounding gas mixture is given below (for details of derivation, refer to ref 31)

$$\dot{m}L(T_s) = h_{i,\text{eff}}(T_d - T_s)$$
$$+ \frac{\kappa\overline{C}_P\dot{m}}{\exp\left[\frac{2r_o\overline{C}_P\dot{m}}{\lambda Nu} - \frac{[C_A](y_{Fsur} - y_{Fo})}{\lambda}\frac{Sh}{Nu}\right] - 1}(T_{sur} - T_s) \tag{8}$$

where $h_{i,\text{eff}}$ is the effective heat-transfer coefficient of drop interior that considers internal circulation, r_o is the droplet radius, Sh is the Sherwood number, Nu is the Nusselt number, $\overline{C}_P$ is the average specific heat of the gas mixture including fuel vapor, κ is a correlation factor defined by Ra and Reitz,[36] $[C_A]$ is the interdiffusional difference of energy flux between fuel and air, y_{Fo} and y_{Fsur} are the mass fractions of fuel at the interface and far away, respectively, and T_{sur} is the surrounding gas temperature.

The rate of mass transport at the droplet surface is calculated using the well-known high mass-transfer rate equation with Spalding's transfer number[37]

$$\dot{m} = g_m \ln(1 + B_M) \tag{9}$$

where g_m is the mass-transfer coefficient determined from $g_m = Sh\rho\overline{D}/2R$ and B_M is Spalding's transfer number, $(y_{Fs} - y_{Fsur})/(1 - y_{Fs})$.

For boiling evaporation, the surface temperature in eq 8 becomes equal to the boiling temperature ($T_s = T_b$) corresponding to the ambient gas pressure and the droplet composition and the surface fuel mass fraction becomes unity ($y_{Fo} = 1$). Note that Spalding's transfer number becomes invalid at the boiling condition, so that the evaporation rate is determined by the energy balance equation.

$$\dot{m}L(T_b) = \alpha(T_d - T_b)$$
$$+ \frac{\kappa\overline{C}_P\dot{m}}{\exp\left[\frac{2r_o\overline{C}_P\dot{m}}{\lambda Nu} - \frac{[C_A](y_{Fsur} - 1)}{\lambda}\frac{Sh}{Nu}\right] - 1}(T_{sur} - T_b) \tag{10}$$

Here, α is an effective heat-transfer coefficient that considers the contribution of heat transfer by internal circulation at the saturation temperature and the heat-transfer enhancement through the effect of nucleation.

The vaporization rate determined from the energy and mass-transfer equations (for normal evaporation cases) is used to calculate the source terms for the vapor-phase transport equations (eq 5).

3.5. Vapor−Liquid Equilibrium. The equilibrium at the interface between the liquid droplet and the surrounding gas is based on the assumption that the chemical potential μ for the liquid phase, l, and the vapor phase, v, are equal for each species i. Assuming an ideal solution, the surface mass fraction of fuel vapor can be determined using Raoult's law. For a mixture of discrete components, Raoult's law is

$$p_{i,v} = x_{i,v}P = x_{i,l}P_{sat,i} \tag{11}$$

where p_i is the partial pressure of species i in the vapor phase at the droplet surface, $P_{sat,i}(T)$ is the vapor pressure of species i at temperature T, x is the mole fraction, and the subscripts v and l denote the vapor and liquid phases, respectively. The species vapor pressure is given by the Clausius−Clapeyron equation.

In the present study, the assumption of ideal solution was applied throughout the calculations. However, to confirm the validity of the ideal solution assumption, simulations of evaporation considering the non-ideal behavior of mixtures were performed by the universal functional activity coefficient (UNIFAC) method.[38,39] To incorporate the non-

Table 3. Surrogate Compositions of FACE Fuels

surrogate hydrocarbons	molecular formula[a]	surrogate mass fractions of FACE fuels								
		1	2	3	4	5	6	7	8	9
n-decane	$C_{10}H_{22}$ (PC)	0.000	0.000	0.000	0.000	0.100	0.000	0.161	0.000	0.050
n-dodecane	$C_{12}H_{26}$ (PC)	0.162	0.090	0.000	0.000	0.000	0.000	0.090	0.027	0.000
n-tridecane	$C_{13}H_{28}$ (PC)	0.000	0.000	0.000	0.050	0.166	0.000	0.000	0.000	0.000
n-tetradecane	$C_{14}H_{30}$ (PC)	0.000	0.000	0.000	0.000	0.130	0.099	0.100	0.169	0.050
n-hexadecane	$C_{16}H_{34}$ (PC)	0.000	0.000	0.080	0.050	0.060	0.198	0.102	0.122	0.181
n-octadecane	$C_{18}H_{38}$ (PC)	0.101	0.020	0.040	0.070	0.071	0.091	0.041	0.051	0.000
n-eicosane	$C_{20}H_{42}$ (PC)	0.000	0.050	0.000	0.000	0.000	0.000	0.000	0.000	0.061
n-heneicosane	$C_{21}H_{44}$ (PC)	0.000	0.050	0.000	0.080	0.000	0.080	0.000	0.046	0.000
2,2,3,3-tetramethylhexane	$C_{10}H_{22}$ (IP)	0.260	0.367	0.095	0.051	0.000	0.000	0.000	0.000	0.000
2,2,4,4,6,8,8-heptamethylnonane	$C_{16}H_{34}$ (IP)	0.100	0.070	0.100	0.110	0.000	0.000	0.000	0.000	0.000
cyclohexane	C_6H_{12} (MCP)	0.030	0.030	0.050	0.060	0.020	0.010	0.020	0.010	0.080
decalin	$C_{10}H_{18}$ (DCP)	0.120	0.120	0.200	0.160	0.270	0.314	0.140	0.162	0.260
m-xylene	C_8H_{10} (AB)	0.000	0.010	0.020	0.000	0.007	0.000	0.000	0.000	0.010
tetralin	$C_{10}H_{12}$ (AB)	0.008	0.007	0.075	0.006	0.029	0.060	0.000	0.040	0.069
naphthalene	$C_{10}H_8$ (PA)	0.015	0.012	0.058	0.000	0.010	0.000	0.024	0.111	0.000
phenanthrene	$C_{14}H_{10}$ (PA)	0.000	0.000	0.000	0.017	0.000	0.050	0.000	0.169	0.055
m-cymene	$C_{10}H_{14}$ (AB)	0.152	0.130	0.180	0.246	0.034	0.000	0.060	0.000	0.020
n-pentylbenzene	$C_{11}H_{16}$ (AB)	0.042	0.033	0.052	0.000	0.032	0.000	0.062	0.000	0.040
n-hexylbenzene	$C_{12}H_{18}$ (AB)	0.000	0.000	0.000	0.000	0.021	0.000	0.040	0.022	0.000
n-heptylbenzene	$C_{13}H_{20}$ (AB)	0.010	0.010	0.050	0.100	0.050	0.098	0.160	0.070	0.124
number of surrogate species		11	14	12	12	14	9	12	12	12

[a] PC, normal paraffin; IP, isoparaffin; MCP, monocycloparaffin; DCP, dicycloparaffin; PA, polynuclear aromatic; AB, alkylbenzene.

ideal mixing effect, the vapor pressure, $p_{i,v}$, is corrected by an activity coefficient, γ_i, of the component in the multi-component liquid mixture that is determined from the UNIFAC method as

$$p_{i,v} = x_{i,v}P = x_{i,1}\gamma_i P_{sat,i} \qquad (12)$$

3.6. Calculation of Distillation Curve. In the present work, the evaporation of a single stagnant droplet at ambient pressure of 1 atm is modeled to simulate the batch distillation process. The schematic configuration of the temperature and heat flux profiles in distillation is shown in Figure 3a, and the corresponding model conditions of a boiling droplet are shown in Figure 3b. With an assumption of the uniform distributions of the component in the drop interior, a droplet of multi-component fuel under a flash boiling vaporization process can successfully simulate the batch distillation process, where $T_d > T_b$. The vaporized fuel components are assumed to mix instantaneously and perfectly with the surrounding ambient gases; thus, no mass-transport phenomenon in the gas phase around the droplet is involved in the distillation process. During the evaporation process, the drop conditions, including the drop surface temperature (saturation temperature), the ambient gas temperature, the species mass fractions of the drop interior and surface, the ambient fuel mass fraction, and the drop size and mass, are monitored.

Assuming a spherical droplet over the entire evaporation period, the evaporated amount is obtained from the remaining mass. The volume of vaporized fuel condensed back into the liquid phase, V_{distil}, is calculated using the density of each component at the reference temperature. In comparison to the initial liquid mixture volume, V_o, the fraction of liquid volume recovered is given as

$$Vol_{rec} = (1 - V_{distil}/V_o) \times 100 \qquad (13)$$
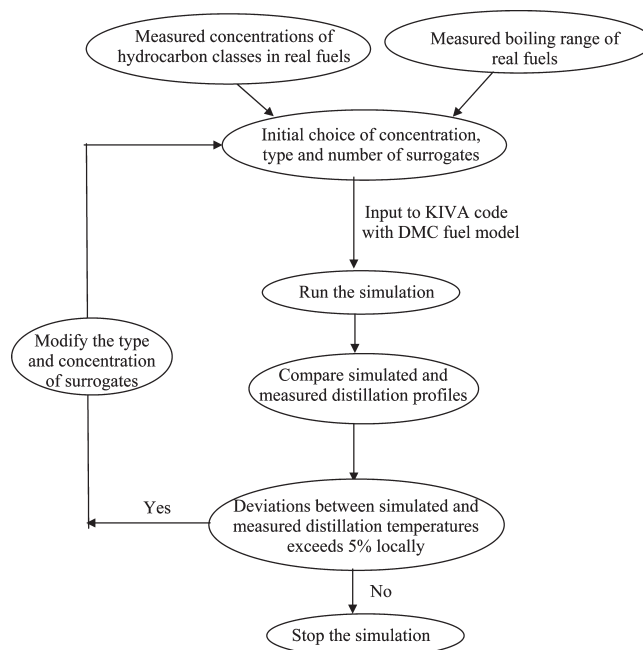

Figure 4. Flowchart showing the surrogate formulation method.

Note that, by tracking the drop surface temperature which is equal to the boiling (saturation) temperature corresponding to the drop composition, the computed distillation curve indicates the profile of the true boiling point (TBP). However, some of the possible sources of error/offset between the present model and the ASTM D86
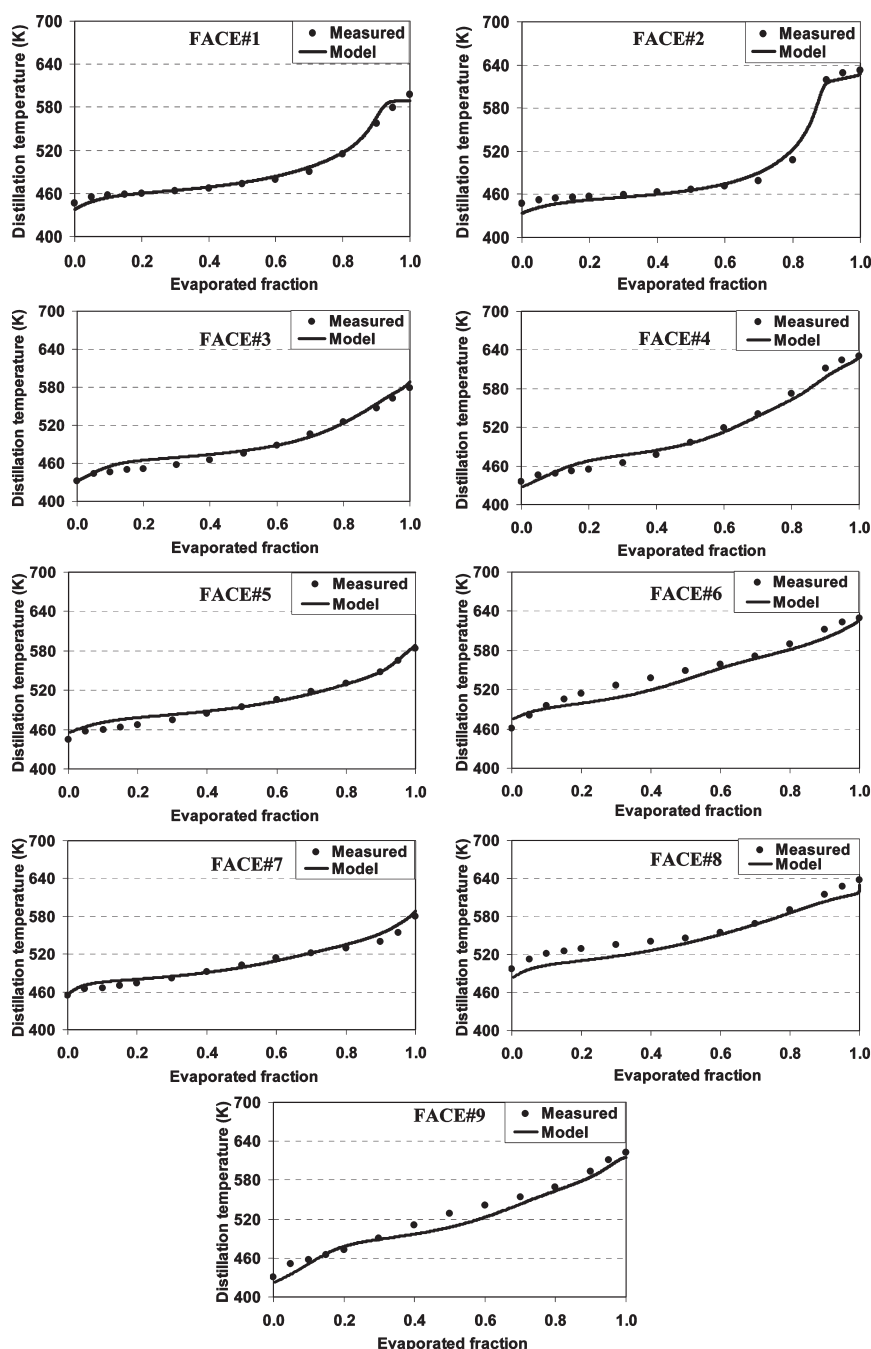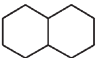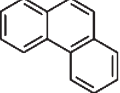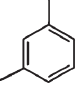
Figure 5. Comparison of measured and predicted distillation profiles of FACE fuels.

distillation measurement, which are ignored in the model, are as follows: (i) in the distillation measurement, there may be a marginal loss of the evaporated fraction during its flow from the point of evaporation to the recovery point; (ii) there is a temperature lag in the experiment because the measuring point is not the liquid/vapor surface, while the calculated boiling temperature is at the interface, which is given by the composition and ambient pressure only; and (iii) there is error in the calculation of liquid mixture properties, especially density.
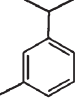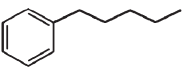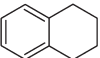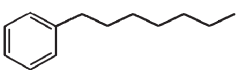
The 20 surrogate hydrocarbon species shown in Table 3 were considered in the study. They were selected because their classes, boiling ranges, and properties span the ranges of the FACE fuels and thermo-chemical data are available for those species. The optimum surrogate compositions for all of the fuels were arrived at through a manual iterative process. The initial choice of the concentrations, type, and number of surrogates for each fuel from the database of 20 surrogate components was made based on the measured concentrations of the hydrocarbon classes and the measured boiling range of the nine fuels. The KIVA code with the DMC fuel model was run, and the simulated distillation profile was compared to the measured data. The initial concentrations of the surrogates were modified whenever the deviations between the simulated and measured distillation temperatures exceed 5%. The manual iterative process was repeated, and the code was run with modified surrogate concentrations until there was a good agree-ment between the simulated and measured distillation temperatures. The measured concentrations of the hydrocarbon classes were

Table 4. Chemical Structure and Activity Coefficients of Surrogates in FACE 9

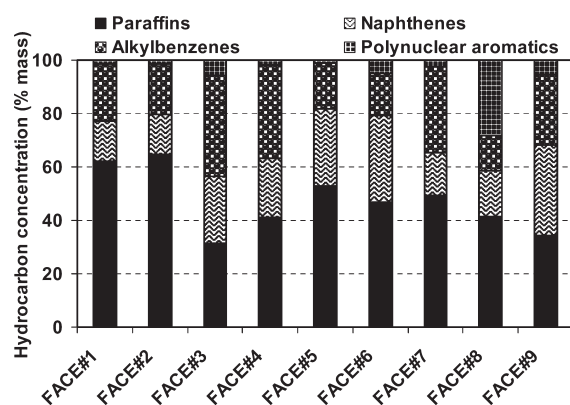| component	chemical structure	activity coefficient at 373 K
n-Tetradecane ($C_{14}H_{30}$)		1.01
Cyclohexane (C_6H_{12})		0.88
Decalin ($C_{10}H_{18}$)		1.03
n-Decane ($C_{10}H_{22}$)		1.06
n-Hexadecane ($C_{16}H_{34}$)		0.95
n-Eicosane ($C_{20}H_{42}$)		0.81
Phenanthrene ($C_{14}H_{10}$)		2.22
m-Xylene (C_8H_{10})		1.06
m-Cymene ($C_{10}H_{14}$)		1.07
Pentylbenzene ($C_{11}H_{16}$)		1.08
Tetralin ($C_{10}H_{12}$)		1.17
Heptylbenzene ($C_{13}H_{20}$)		1.10

Figure 6. Hydrocarbon class distribution in FACE surrogates.

maintained throughout the process to match the measured boiling range. The surrogate formulation method is summarized in Figure 4.
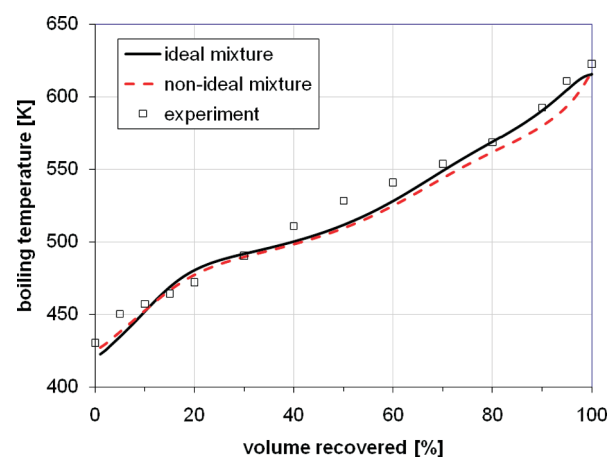

Figure 7. Comparison of distillation curves between the cases with and without non-ideality calculation. FACE 9 model fuel was simulated.
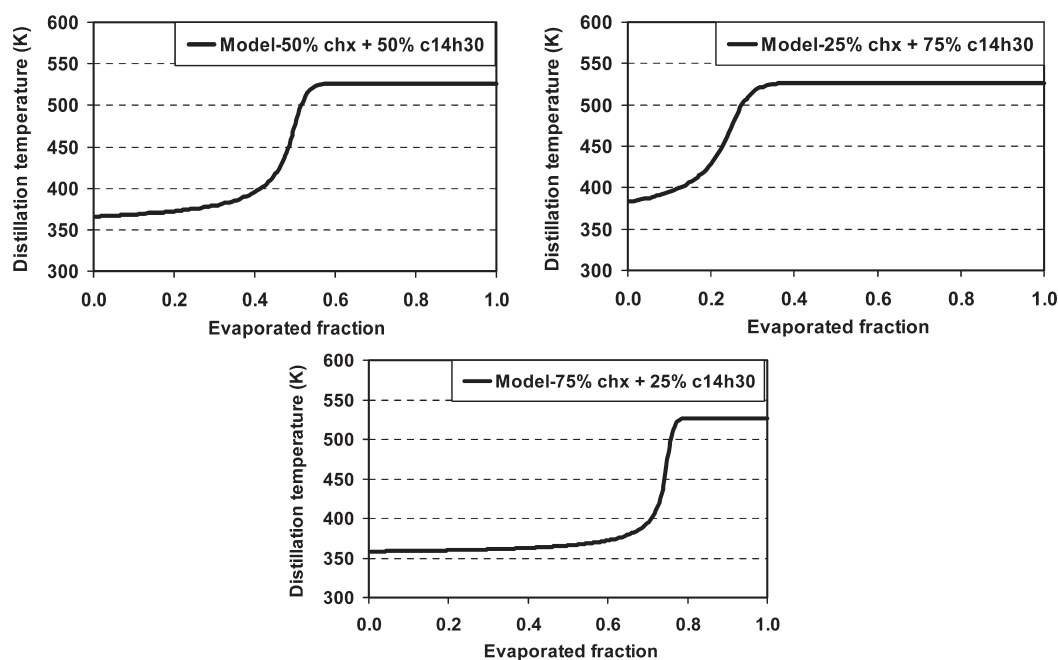
Figure 8. Distillation characteristics of a binary mixture.

Table 5. Summary of Estimated and Measured[7] Properties of FACE Fuels

fuel FACE	specific gravity			lower heating value (MJ/kg)			H/C ratio			cetane number		
	estimated	measured	error (%)	estimated	measured	error (%)	estimated	measured	error (%)	estimated	measured	error (%)
1	0.804	0.808	−0.5	43.24	42.77	1.1	1.96	1.99	−1.5	38.3	35.3	8.5
2	0.802	0.803	−0.1	43.31	43.13	0.4	1.98	1.92	3.1	36.4	34.6	5.2
3	0.850	0.840	1.2	42.37	42.12	0.6	1.75	1.86	−6.1	29.7	33.8	−12.1
4	0.825	0.836	−1.3	42.75	42.47	0.7	1.85	1.80	2.5	41.2	32.9	25.2
5	0.819	0.808	1.4	43.15	42.87	0.7	1.94	1.92	1.1	64.4	54.9	17.3
6	0.841	0.841	0.0	42.82	42.77	0.1	1.88	1.90	−1.1	67.3	53.6	25.6
7	0.812	0.837	−3.0	42.99	42.33	1.6	1.87	1.85	1.3	57.7	45.4	27.1
8	0.865	0.869	−0.4	41.90	42.17	−0.6	1.64	1.70	−3.3	52.6	50.2	4.8
9	0.843	0.846	−0.4	42.60	42.44	0.4	1.79	1.79	0.1	51.5	44.6	17.7

fuel FACE	cetane index			distillation temperature (K)								
				T_{10}			T_{50}			T_{90}		
	estimated	measured	error (%)	estimated	measured	error (%)	estimated	measured	error (%)	estimated	measured	error (%)
1	43.7	40.1	9.0	454	457	−0.7	475	473	0.4	565	557	1.4
2	40.7	39.0	4.2	447	454	−1.5	466	466	0.0	614	619	−0.8
3	29.1	31.2	−6.7	456	446	2.2	480	475	1.1	554	547	1.3
4	43.3	40.7	6.4	451	449	0.4	495	496	−0.2	598	611	−2.1
5	45.2	49.7	−9.1	471	459	2.6	494	494	0.0	548	548	0.0
6	49.1	52.1	−5.8	492	496	−0.8	535	548	−2.4	599	612	−2.1
7	49.7	41.9	18.5	476	466	2.1	499	503	−0.8	553	540	2.4
8	42.1	42.9	−1.9	503	521	−3.5	538	546	−1.5	603	615	−2.0
9	41.2	46.1	−10.6	451	457	−1.3	508	528	−3.8	585	593	−1.3

3.7. Surrogate Fuel Property Estimation. Examination of the data in Figure 2 reveals that different sets of hydrocarbons can describe the boiling range of a particular FACE fuel. Hence, it was necessary to judge the suitability of the chosen surrogate compositions by comparing their other important properties against measured data as well. For this purpose, the specific gravity, lower heating value, hydrogen/carbon (H/C) ratio, and cetane number of the surrogate fuels were estimated on the basis of their composition and property data available in the
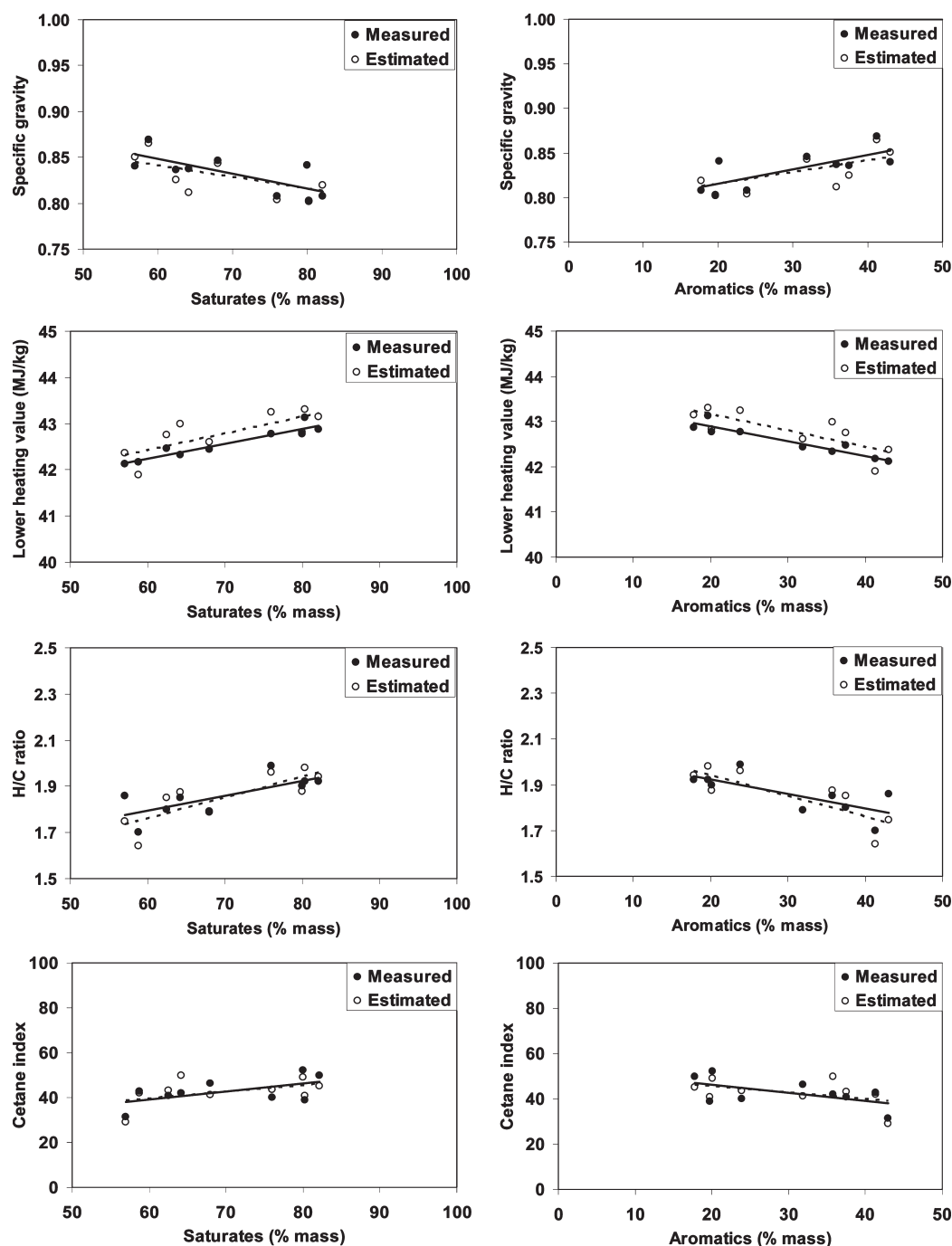
Figure 9. Variations in FACE fuel properties with changes in composition.

literature. The H/C ratio of the surrogate fuels is specified by their molecular formula. The specific gravity and the lower heating values were taken from Daubert and Danner,[34] and the cetane number data was obtained from refs 26, 40, and 41. Because of the non-availability of measured cetane number data for n-heneicosane, it is assumed to be equal to 110, considering the fact that the measured cetane number data for the n-paraffins with carbon numbers 18−20 are equal to 110. The surrogate mixture properties were calculated on the basis of the assumption of linear blending of the pure component properties. Although this linear blending assumption is found to give reasonable accuracy for the estimation of specific gravity and heating values,[16] it can be less accurate for cetane number estimation because of nonlinear

behavior and interactions between certain classes of hydrocarbons, such as paraffins and naphthenes.[25,42] However, the number of interaction parameters required to describe this nonlinear behavior increases significantly with an increase in the number of hydrocarbon classes.[42] Previous research has shown that the cetane number estimation of hydrocarbon mixtures based on a linear blending assumption can be adequate and provides reasonable agreement with measured data.[1]

4. RESULTS AND DISCUSSION

The predicted distillation profiles of the nine fuels are compared to the measured data in Figure 5. It is observed that

the initial, final, and mid-boiling ranges of all of the fuels are captured well in the simulations, with a maximum absolute error of ~4%. The final surrogate compositions of the fuels are provided in Table 3, and the hydrocarbon class distribution in FACE surrogates are shown in Figure 6. The optimum number of surrogate components required to obtain a good agreement of the distillation profiles varied between 9 (for FACE 6) and 14 (for FACE 2 and 5). A comparison of the surrogate compositions with the measured hydrocarbon classes given in Table 2 shows that the measured concentrations of paraffins, total naphenes, total saturates, polynuclear aromatics, alkylbenzenes, tetralin, and total aromatics are also maintained well in the surrogate compositions of all of the nine fuels. A good agreement between the simulated and measured distillation temperatures was achieved while retaining the actual split between chemistry classes.

To investigate the influence of the possible molecular interaction in the mixture, i.e., non-ideality of the mixture on the vaporization process, the distillation curve of the FACE 9 fuel obtained using the UNIFAC method was compared to that obtained using the ideal mixture assumption. The chemical structure of the components considered in FACE 9 fuel and their activity coefficient at 373 K (refer to eq 12) are listed in Table 4. Most of the components do not show significant deviation of the activity coefficient from unity. However, it is interesting that phenanthrene, which is a polyaromatic hydrocarbon, has a relatively large activity coefficient, which implies that it may contribute to the deviation of the distillation curve at the high boiling temperatures.

Figure 7 shows a comparison of distillation curves between the cases with and without non-ideality calculation. Over the early and intermediate period of the distillation, the effects of the molecular interaction among the components are very minor. It is interesting that the deviation of the distillation curve from that of the ideal mixture case slightly increases as the evaporation approaches the end of the distillation process. As discussed above, this is attributed to the high activity coefficient of phenanthrene, which is expected to vaporize at high temperatures during the later phase of the distillation process. Overall, it is seen that the two distillation curves are in good agreement over the entire period of distillation. Note that, for the other fuel models, the discrepancy of the distillation curves between the ideal and non-ideal mixture models (not shown here) was much less than that for the FACE 9 fuel, which justifies the use of the ideal mixture assumption in the evaporation calculations for the fuels considered in the present study. Also, it is to be noted that there is no stepwise behavior and the distillation profiles are obtained as smooth curves, as shown in Figure 5. To verify that the process could reproduce a stepped distillation behavior, the code is run with varying fractions of a binary mixture of cyclohexane and tetradecane and it is observed that a smooth curve is obtained until the lower boiling point component is completely evaporated, as shown in Figure 8, which augments the trends of distillation profiles of FACE fuels, which are smooth curves.

From the surrogate compositions and the hydrocarbon property data, the specific gravity, lower heating value, H/C ratio, and cetane number of the nine fuels were estimated and compared to the measured data,[7] as shown in Table 5. A comparison of the 10, 50, and 90% distillation temperatures with the measured data is also provided in Table 5. It is observed that the specific gravity, lower heating value, H/C ratio, and distillation temperature predictions for all nine fuels are in good agreement with the measured data, with maximum absolute error values of ~3, ~1.6, ~6, and ~4%, respectively. The higher prediction error observed for cetane number matching in Table 5 could be possibly due to the linear blending assumption. To address this problem, the cetane index values of the nine fuels were also estimated on the basis of the ASTM D976 test, which requires density and 50% distillation temperature values as inputs. A comparison of the estimated cetane index to the measured data in Table 5 shows good agreement with only a ~10% maximum absolute error (except for FACE 7). The poorer agreement between the measured and estimated cetane number/cetane index values for FACE 7 may be partially due to its significantly lower measured cetane number compared to its target cetane number value.[7]

To examine the effect of composition variations on the fuel properties, the estimated and measured specific gravity, lower heating value, H/C ratio, and cetane index of the fuels are compared to their saturate and aromatic contents in Figure 9. It is observed that these property values show opposite trends with an increase in their saturate and aromatic contents. The lower heating value, H/C ratio, and cetane index are found to increase, and the specific gravity decreases, with an increase in saturate contents of the fuels. A higher molar volume of the saturates compared to their aromatic counterpart decreases the specific gravity. The variations in the heating value of the fuels with composition correlates well with changes in their H/C ratio, with an increase in the H/C ratio increasing the heating value. An increase in the cetane index with an increase in the saturate content signifies the better ignitability of the saturates, as compared to the aromatics, which is well-known.

5. CONCLUSIONS

The following conclusions are drawn from the present work on the development of surrogates for the physical properties of the FACE fuels: (i) An accurate simulation of the distillation profiles of real fuels is found to be an effective tool for modeling their composition and physical properties using representative "physical property" surrogate components. (ii) However, for accurate representation of the physical properties of the fuel, a fairly large number of surrogate components are required (~14 species). Thus, a non-hybrid approach may provide surrogates that are too large or complex for practical chemistry modeling, and therefore, a hybrid approach that uses fewer surrogate species to represent the chemistry (but which includes the same classes of hydrocarbon species in the surrogate composition) might be needed for practical combustion models. (iii) The present surrogate models were found to be adequate for representing the physical properties of the real fuels. In particular, there is excellent agreement between the predicted and measured specific gravity, lower heating value, and distillation temperatures. Inclusion of lower molecular-weight constituents could further improve the H/C ratio matching for surrogate fuels having lower H/C ratios but at the cost of poorer distillation temperature predictions. Also, the consideration of nonlinearity of the cetane number in the surrogate mixture is expected to improve the cetane number predictions.

■ AUTHOR INFORMATION

Corresponding Author
*E-mail: krishnasamy@wisc.edu.

■ REFERENCES

(1) Androulakis, I. P.; Weisel, M. D.; Hsu, C. S.; Qian, K.; Green, L. A.; Farrell, J. T.; Nakakita, K. *Energy Fuels* **2005**, *19*, 111–119.

(2) Wallington, T. J.; Kaiser, E. W.; Farrell, J. T. *Chem. Soc. Rev.* **2006**, *35*, 335–347.

(3) Bunting, B. G.; Wildman, C. B.; Szybist, J. P.; Lewis, S.; Storey, J. *Int. J. Eng. Res.* **2007**, *8*, 15–27.

(4) Ghazikhani, M.; Kalateh, M. R.; Toroghi, Y. K.; Dehnavi, M. *Int. J. Aerosp. Mech. Eng.* **2010**, *4* (2), 81–87.

(5) Bunting, B. G.; Eaton, S. J.; Crawford, R. W. Performance evaluation and optimization of diesel fuel properties and chemistry in an HCCI engine. *Proceedings of the Society of Automotive Engineers (SAE) 2009 Powertrains Fuels and Lubricants Meeting*; San Antonio, TX, Nov 2009; SAE 2009-01-2645.

(6) Co-ordinating Research Council (CRC). http://www.crcao.com/news/index.html (accessed on Nov 1, 2010).

(7) Gallant, T.; Franz, J. A.; Alnajjar, M. S.; Storey, J. M. E.; Lewis, S. A.; Sluder, C. S.; Cannella, W. J.; Fairbridge, C.; Hager, D.; Dettman, H.; Luecke, J.; Ratcliff, M. A.; Zigler, B. T. Fuels for advanced combustion engines research diesel fuels: Analysis of physical and chemical properties. *Proceedings of the Society of Automotive Engineers (SAE) 2009 Powertrains Fuels and Lubricants Meeting*, San Antonio, TX, Nov 2009; SAE 2009-01-2769.

(8) Alnajjar, M.; Cannella, B.; Dettman, H.; Fairbridge, C.; Franz, J.; Gallant, T.; Gieleciak, R.; Hager, D.; Lay, C.; Lewis, S.; Ratcliff, M.; Sluder, S.; Storey, J.; Yin, H.; Zigler, B. *Chemical and Physical Properties of the Fuels for Advanced Combustion Engines (FACE) Research Diesel Fuels*, Report; Oak Ridge National Laboratory, U.S. Department of Energy, July 2010; Contract DE-AC05-00OR22725.

(9) Cho, K.; Han, M.; Sluder, C. S.; Wagner, R. M.; Lilik, G. K. Experimental investigation of the effects of fuel characteristics on high efficiency clean combustion in a light-duty diesel engine. *Proceedings of the Society of Automotive Engineers (SAE) 2009 Powertrains Fuels and Lubricants Meeting*, San Antonio, TX, Nov 2009; SAE 2009-01-2669.

(10) Amsden, A. A. *KIVA-3V, Release 2, Improvements to KIVA-3V*; Los Alamos National Laboratory: Los Alamos, NM, 1999; Report LA-UR-99-915.

(11) Ranzi, E. *Energy Fuels* **2006**, *20*, 1024–1032.

(12) Hernandez, J. J.; Sanz-Argent, J.; Benajes, J.; Molina, S. *Fuel* **2008**, *87*, 655–665.

(13) Cathonnet, M. *Proceedings of the European Combustion Meeting*; Orleans, France, Oct 20–23, 2003.

(14) Pitz, W. J.; Mueller, C. J. *Prog. Energy Combust. Sci.* **2010**, 1–21.

(15) Farrell, J. T.; Cernansky, N. P.; Dryer, F. L.; Law, C. K.; Friend, D. G.; Hergart, C. A.; McDavid, R. M.; Patel, A. K.; Mueller, C. J.; Pitsch, H.; Development of an experimental database and kinetic models for surrogate diesel fuels. *Proceedings of the Society of Automotive Engineers (SAE) World Congress and Exhibition*; Detroit, MI, April 2007; SAE 2007-01-0201.

(16) Naik, C. V.; Puduppakkam, K.; Wang, C.; Kottalam, J.; Liang, L.; Hodgson, D.; Meeks, E. Applying detailed kinetics to realistic engine simulation: The surrogate blend optimizer and mechanism reduction strategies. *Proceedings of the Society of Automotive Engineers (SAE) 2010 World Congress and Exhibition*; Detroit, MI, April 2010; SAE 2010-01-0541.

(17) Mensch, A.; Santoro, R. J.; Litzinger, T. A.; Lee, S. Y. *Combust. Flame* **2010**, *157*, 1097–1105.

(18) Huber, M. L.; Lemmon, E. W.; Bruno, T. J. *Energy Fuels* **2010**, *24*, 3565–3571.

(19) Colket, M.; Edwards, T.; Williams, S.; Cernansky, N. P.; Miller, D. L.; Egolfopoulos, F.; Dryer, F. L.; Bellan, J.; Lindstedt, P.; Seshadri, K.; Pitsch, H.; Sarofim, A.; Smooke, M.; Tsang, W. Identification of target validation data for development of surrogate jet fuels. *Proceedings of the 46th American Institute of Aeronautics and Astronautics (AIAA) Aerospace Sciences Meeting and Exhibit*; Reno, NV, Jan 7–10, 2008; Paper AIAA 2008-972.

(20) Slavinskaya, N. A.; Zizin, A.; Aigner, M. *J. Eng. Gas Turbines Power* **2010**, *132*, 1–10.

(21) Liang, L.; Naik, C. V.; Puduppakkam, K.; Wang, C.; Modak, A.; Meeks, E.; Ge, H.-W.; Reitz, R.; Rutland, C. Efficient simulation of diesel engine combustion using realistic chemical kinetics in CFD. *Proceedings of the Society of Automotive Engineers (SAE) 2010 World Congress and Exhibition*; Detroit, MI, April 2010; SAE 2010-01-0178.

(22) Natelson, R. H.; Kurman, M. S.; Cernansky, N. P.; Miller, D. L. *Fuel* **2008**, *87*, 2339–2342.

(23) Ra, Y.; Reitz, R. D. *Combust. Flame* **2011**, *158*, 69–90.

(24) Ra, Y.; Reitz, R. D.; McFarlane, J.; Daw, C. S. Effects of fuel physical properties on diesel engine combustion using diesel and bio-diesel fuels. *Proceedings of the Society of Automotive Engineers (SAE) World Congress and Exhibition*; Detroit, MI, April 2008; SAE 2008-01-1379.

(25) Agosta, A. M.S. Thesis, Department of Mechanical Engineering and Mechanics (MEM), Drexel University, Philadelphia, PA, May 2002.

(26) Rose, J. W.; Cooper, J. R. *Technical Data on Fuel*, 7th ed.; John Wiley and Sons: New York, 1977.

(27) Puduppakkam, K. V.; Kokjohn, S. L.; Liang, L.; Naik, C. V.; Reitz, R. D.; Meeks, E. Use of detailed kinetics and advanced chemistry-solution techniques in CFD to investigate dual-fuel engine concepts. *Proceedings of the THIESEL 2010 Conference on Thermo- and Fluid Dynamic Processes in Diesel Engines*; Valencia, Spain, Sept 13–16, 2010.

(28) Naik, C. V.; Pitz, W. J.; Westbrook, C. K.; Sjöberg, M.; Dec, J. E.; Orme, J.; Curran, H. J.; Simmie, J. M. Detailed chemical kinetic modeling of surrogate fuels for gasoline and application to an HCCI engine. *Proceedings of the Powertrain and Fluid Systems Conference and Exhibition*; San Antonio, TX, Oct 2005; SAE 2005-01-3741.

(29) Pitz, W. J.; Cernansky, N. P.; Dryer, F. L.; Egolfopoulos, F. N.; Farrell, J. T.; Friend, D. G.; Pitsch, H. Development of an experimental database and kinetic models for surrogate gasoline fuels. *Proceedings of the 2007 Society of Automotive Engineers (SAE) World Congress*; Detroit, MI, 2007; SAE 2007-01-0175.

(30) Owen, K.; Coley, T. *Automotive Fuels Reference Book*, 2nd ed.; Society of Automotive Engineers (SAE): Warrendale, PA, 1995.

(31) Ra, Y.; Reitz, R. D. *Int. J. Multiphase Flow* **2009**, *35*, 101–117.

(32) Abani, N.; Kokjohn, S.; Park, S. W.; Bergin, M.; Munnannur, A.; Ning, W.; Sun, Y.; Reitz, R. D. An improved spray model for reducing numerical parameter dependencies in diesel engine CFD simulations. *Proceedings of the Society of Automotive Engineers (SAE) World Congress and Exhibition*; Detroit, MI, April 2008; SAE 2008-01-0970.

(33) Kee, R. J.; Rupley, F. M.; Miller, J. A. *CHEMKIN-II: A FORTRAN Chemical Kinetics Package for the Analysis of Gas Phase Chemical Kinetics*; Sandia National Laboratories: Albuquerque, NM, 1989; Sandia Report SAND 89-8009.

(34) Daubert, T. E.; Danner, R. P. *Physical and Thermodynamic Properties of Pure Chemicals*; Taylor and Francis Group: London, U.K., 1997; Vol. 4 and 5.

(35) Abdel-Qadera, Z.; Hallett, W. L. H. *Chem. Eng. Sci.* **2005**, *60*, 1629–1640.

(36) Ra, Y.; Reitz, R. D. *Int. J. Eng. Res.* **2003**, *4*, 193–218.

(37) Sirignano, W. A. *Prog. Energy Combust. Sci.* **1983**, *9*, 291–322.

(38) Fredenslund, A.; Jones, R. M.; Prausnitz, J. M. *Supplement to Program UNIFAC-Group Contribution Estimation of Activity Coefficients in Non-ideal Liquid Mixtures*, Report; University of California: Berkeley CA, 1974.

(39) Jiao, Q.; Ra, Y.; Reitz, R. D. Submitted to *Society of Automotive Engineers (SAE) World Congress 2011*; Detroit, MI, April 12–14, 2011.

(40) Murphy, M. J.; Taylor, J. D.; McCormick, R. L. *Compendium of Experimental Cetane Number Data*, Technical Report; National Renewable Energy Laboratory (NREL), U.S. Department of Energy (DOE): Golden, CO, Sept 2004; Contract DE-AC36-99-GO10337.

(41) Do, P. T. M.; Crossley, S.; Santekunaporn, M.; Resasco, D. E. *Catalysis* **2007**, *20*, 33–64.

(42) Ghosh, P.; Hickey, K. J.; Jaffe, S. B. *Ind. Eng. Chem. Res.* **2006**, *45*, 337–345.